

Excitonic Effects and Optical Spectra of Single-Walled Carbon Nanotubes

Catalin D. Spataru,^{1,2} Sohrab Ismail-Beigi,^{1,2} Lorin X. Benedict,³ and Steven G. Louie^{1,2}

¹*Department of Physics, University of California at Berkeley, Berkeley, California 94720*

²*Materials Sciences Division, Lawrence Berkeley National Laboratory, Berkeley, California 94720*

³*H Division, Physics and Advanced Technologies Directorate,*

Lawrence Livermore National Laboratory, University of California, Livermore, CA 94550

(Dated: November 5, 2018)

Many-electron effects often dramatically modify the properties of reduced dimensional systems. We report calculations, based on an *ab initio* many-electron Green's function approach, of electron-hole interaction effects on the optical spectra of small-diameter single-walled carbon nanotubes. Excitonic effects qualitatively alter the optical spectra of both semiconducting and metallic tubes. Excitons are bound by ~ 1 eV in the semiconducting (8,0) tube and by ~ 100 meV in the metallic (3,3) tube. These large many-electron effects explain the discrepancies between previous theories and experiments.

Synthesis and observation of single-walled carbon nanotubes (SWCNT) have advanced greatly in recent years, making possible the experimental study of the optical properties of individual SWCNTs [1, 2]. If well understood, the optical response of SWCNTs may be used to characterize these nanotubes, to monitor and guide their separation by type [3], and can be employed in device applications [4]. However, measured optical transition frequencies deviate substantially from theoretical predictions based on one-particle interband theories. This deviation is not unexpected since many-body interactions should play a vital role in reduced dimensions [5]. Our *ab initio* results show that, indeed, many-electron effects can change qualitatively the optical spectra of SWCNTs. Strongly bound excitons are predicted in small diameter semiconducting nanotubes and even in some metallic tubes, and they dominate the optical response.

Below, motivated by recent experiments [1, 3], we compute the optical absorption spectra of the three small-diameter SWCNTs: (3,3), (5,0), and (8,0). We use a recently developed approach in which electron-hole excitations and optical spectra of real materials are calculated from first principles in three stages [6]: (i) we treat the electronic ground-state with *ab initio* pseudopotential density-functional theory (DFT) [7], (ii) we obtain the quasiparticle energies $E_{n\mathbf{k}}$ within the *GW* approximation for the electron self-energy Σ [8] by solving the Dyson equation:

$$\left[-\frac{\nabla^2}{2} + V_{ion} + V_{Hartree} + \Sigma(E_{n\mathbf{k}}) \right] \psi_{n\mathbf{k}} = E_{n\mathbf{k}} \psi_{n\mathbf{k}} ,$$

and (iii) we calculate the coupled electron-hole excitation energies Ω^S and spectrum by solving the Bethe-Salpeter equation of the two-particle Green's function [6, 9]:

$$(E_{c\mathbf{k}} - E_{v\mathbf{k}}) A_{v\mathbf{c}\mathbf{k}}^S + \sum_{\mathbf{k}'v'c'} \langle v\mathbf{c}\mathbf{k} | K^{eh} | v'c'\mathbf{k}' \rangle A_{v'c'\mathbf{k}'}^S = \Omega^S A_{v\mathbf{c}\mathbf{k}}^S ,$$

where $A_{v\mathbf{c}\mathbf{k}}^S$ is the exciton amplitude, K^{eh} is the electron-hole interaction kernel, and $|c\mathbf{k}\rangle$ and $|v\mathbf{k}\rangle$ are the quasi-electron and quasihole states, respectively. We obtain

the DFT wavefunctions and eigenvalues by solving the Kohn-Sham equations within the local density approximation (LDA) [7] using a plane-wave basis with an energy cutoff of 60 Ry. We use *ab initio* Troullier-Martins pseudopotentials [10] in the Kleinmann-Bylander form [11] ($r_c = 1.4$ a.u.). To compare with experiments in which 4 Å diameter SWCNTs are grown inside zeolites [1], we study the (3,3) and (5,0) tubes in the experimental geometry with a dielectric background of $AlPO_4$ [12]. For the (8,0) tube, we work in a supercell with an intertube separation of at least 9.7 Å to mimic experiments on isolated tubes [2, 3]. In supercells, due to the long range of the screened Coulomb interaction in semiconducting tubes, unphysical interactions between periodic images can lead to deviations from the isolated case. Hence, we truncate the Coulomb interaction in a cylindrical geometry for the semiconducting tubes (we find negligible tube-tube interactions or image effects for metallic tubes where screening is complete). Due to depolarization effects in nanotubes [13], strong optical response is observed only for light polarized along the tube axis (\hat{z}). We only consider this polarization below.

For the metallic tubes (3,3) and (5,0), we find quasiparticle *GW* corrections to the LDA band energies similar to those in graphite, namely a $\sim 15\%$ stretching of the LDA eigenvalues away from the Fermi level (E_F) [14]. While this result is expected for large diameter metallic nanotubes which resemble a graphene sheet, we find it also holds for these small diameter metallic tubes where curvature effects lead to strong $\sigma - \pi$ hybridization [15].

Fig. 1a shows the quasiparticle density of states (DOS) for the metallic (3,3) tube featuring a number of prominent one-dimensional (1D) van Hove singularities (vHs) near E_F . Unlike predictions from simple tight-binding models [16], these vHs are asymmetric about E_F due to strong curvature effects. The arrow in the figure indicates optically allowed low-energy transitions. For the (3,3) metallic tube, the bands forming the first vHs below E_F and the second vHs above E_F meet at the Fermi level, but optical transitions between them are

symmetry-forbidden. We calculate $\epsilon_2(\omega)$ in two ways (see Fig. 1b). First, we neglect electron-hole interactions and find the existence of a symmetry gap, i.e. no electron-hole transition with energy below the prominent peak at $\hbar\omega = 3.25$ eV. Second, we include electron-hole interactions and solve the Bethe-Salpeter equation. In general, the electron-hole interaction kernel has two terms: an attractive direct term involving the screened Coulomb interaction and a repulsive exchange term involving the bare Coulomb interaction [6]. Fig. 1b shows that for the (3,3) tube the direct term dominates: one bound exciton is formed with a binding energy of 86 meV and an extent of ~ 50 Å along \hat{z} . The surprising result of having a bound exciton in a metal stems from having the symmetry gap, which is possible for a quasi 1-D system where all \mathbf{k} -states have well-defined symmetry. Also, the existence of a *sole* bound exciton is due to the metallic screening (the screening length is ≈ 3.2 Å): the effective electron-hole interaction along \hat{z} resembles an attractive $\delta(z)$ function, and in 1D, the Hamiltonian $H = -\frac{1}{2m^*} \frac{d^2}{dz^2} - |V_0| \delta(z)$ has a single bound eigenstate.

Fig. 2a shows the quasiparticle band structure for the metallic (5,0) tube. According to the band-folding scheme [16, 17], this tube should be semiconducting. However, curvature effects [15] lead to strong $\sigma - \pi$ hybridization, forcing a band to cross E_F . Arrows in the figure indicate optically allowed interband transitions which give rise to the two peaks, labeled A and B in the optical spectrum in Fig. 2b. When neglecting electron-hole interactions, peak B has a lower intensity than A because the transitions contributing to B do not originate from a band extremum (vHs) but from the crossing at E_F . For this tube, electron-hole interactions do not bind excitons: while the screening length in the (5,0) tube is similar to that of the (3,3) tube, the symmetry of the bands in the (5,0) tube prohibits direct attraction between the electron-hole pairs contributing to peaks A and B. Thus the electron-hole interaction is governed by the repulsive exchange term. This effect, again, is peculiar to nanotubes: in traditional semiconductors, the attractive direct term dominates over the repulsive exchange term. Moreover, when electron-hole interactions are included, the exchange term has a larger effect on peak B and suppresses it greatly.

We now compare our results for the (3,3) and (5,0) tubes to experiments. In the work of Li et al. [1], 4 Å diameter SWCNTs were grown inside zeolite channels, and three main peaks were found in the measured absorption spectra (see Table 1). While 4 Å diameter SWCNTs come in only three chiralities, (3,3), (5,0) and (4,2), it was not possible to assign directly the specific peaks to specific tubes experimentally. As shown in Table 1, our results for the (3,3) and (5,0) tubes are in excellent quantitative agreement with experiment and provide a concrete identification for two of the observed peaks. We conclude that the remaining peak at 2.1 eV is due to

the (4,2) tube (other calculations ignoring electron-hole interactions point to the same conclusion [18, 19, 20]). Moreover, the many-electron suppression of peak B in the (5,0) spectrum explains the absence of any observed feature in the measured spectra at ≈ 2.8 eV.

We now consider the 6.3 Å diameter semiconducting tube (8,0), in which we expect even larger excitonic effects. The (8,0) tube has a calculated LDA minimum band gap of 0.60 eV. Quasiparticle corrections dramatically open the gap to 1.75 eV. This correction is significantly larger than those in bulk semiconductors with similar LDA gaps: we again attribute this to the 1D nature of the SWCNTs which enhances Coulomb effects (as shown in model calculations [5]).

Fig. 3a shows the calculated absorption spectrum for an isolated (8,0) tube. There are three distinct low-energy peaks (labeled A, B, and C) in the non-interacting spectrum. When electron-hole interactions are included, we find far more dramatic excitonic effects than in the metallic cases: each non-interacting peak gives rise to a series of visible exciton lines with large binding energies of 0.99 eV, 0.86 eV and 1.00 eV for the lowest-energy excitons (A'_1 , B'_1 and C'_1 respectively). These binding energies are more than ten times larger than those in bulk semiconductors with similar gaps, and excitonic effects qualitatively change the spectral profile. Again, these effects stem from the long range of the screened Coulomb interaction and the 1D nature of the SWCNTs: e.g., the binding energy of a 1D hydrogenic system is infinite due to the long-range Coulomb interaction [21]. We note that the electron-hole interaction reverses the relative intensity of the first and second prominent optical peaks.

Theory predicts that there are two varieties of excitons in the (8,0) tube: bound excitons with energies below the non-interacting optical gap (A' and B' series) and resonant excitons with energies above the non-interacting optical gap (C' series). Fig. 3b shows the real-space, electron-hole pair probability distribution $|\Phi(\mathbf{r}_e, \mathbf{r}_h)|^2$ as a function of the electron position \mathbf{r}_e for the photoexcited A'_1 bound exciton obtained by fixing the position of the hole \mathbf{r}_h (the black star in the figure) on a carbon π orbital. Fig. 3c and 3d show this correlation more quantitatively for the bound A'_1 and the resonant C'_1 exciton: $|\Phi|^2$ is plotted along \hat{z} after integrating out the electron coordinates in the perpendicular plane. The extent of the bound part of both excitons is ~ 25 Å.

Our results for the (8,0) tube are in excellent agreement with the experimental findings of Bachilo et al. [3, 23]: by performing spectrofluorimetric measurements on various semiconducting SWCNTs, with diameters ranging from 0.62 to 1.31 nm and chiral angle from 3 to 28 degrees, optical transitions were assigned to specific individual (n,m) tubes. While their SWCNT samples did not contain the (8,0) tube, they obtained results for tubes with similar diameter and chirality and provided fits for the first and second optical transition energies (ν_{11} and

ν_{22}) as a function of diameter and chiral angle, which they demonstrate to work well for a wide range of (n,m) values. Their fits provide a ratio of $\nu_{22}/\nu_{11} = 1.17$ for the (8,0) tube. The traditional non-interacting π -orbital only tight-binding model gives a ratio of 2, and the experimental deviation from 2 has been a puzzle [24, 25, 26]. However, as shown in Table 2, our results for ν_{11} and ν_{22} in the (8,0) tube (peaks A'_1 and B'_1) and their ratio are in excellent agreement with the deduced experimental values. The deviation of ν_{22}/ν_{11} from 2 is a consequence of both band-structure and many-electron effects: one needs to include both for a basic and quantitative understanding.

In conclusion, we study the optical absorption spectra of metallic and semiconducting small diameter SWCNTs and obtain excellent agreement with available experimental data. We show that electron-hole interactions (which can be either attractive or repulsive) play a crucial role, especially for semiconducting tubes, in understanding experimental results. Large excitonic features for both semiconducting and metallic tubes are seen to be due to the quasi-1D nature of SWCNTs, and the manner in which they effect the spectra depends strongly on the rotational symmetries of the tubes.

This work was supported by the NSF under Grant #DMR0087088, and the Office of Energy Research, Office of Basic Energy Sciences, Materials Sciences Division of the U.S. Department of Energy (DOE) under Contract #DE-AC03-76SF00098. Computer time was provided at the DOE Lawrence Berkeley National Laboratory (LBNL)'s NERSC center. Portions of this work were performed under the auspices of the DOE by the University of California Lawrence Livermore National Laboratory (LLNL) under contract No. W-7405-Eng-48. Collaborations between LLNL and LBNL were facilitated by the DOE Computational Materials Sciences Network.

Table 1: Peak position and optical transitions in 4 Å SWCNTs.

Nanotube	Theory	Experiment [1]
(5,0)	1.33 eV	1.37 eV
(3,3)	3.17 eV	3.1 eV
(4,2)	-	2.1 eV

Table 2: Lowest two optical transition energies for the (8,0) SWCNT.

Transition	Theory	Deduced from experiment [3, 23]
ν_{11}	1.55 eV	1.60 eV
ν_{22}	1.80 eV	1.88 eV
ν_{22}/ν_{11}	1.16	1.17

-
- [1] Z.M. Li et al., Phys. Rev. Lett. **87** 127401 (2001).
 [2] M.J. O'Connell et al., Science **297**, 593 (2002).
 [3] S.M. Bachilo et al., Science **298**, 2361 (2002).
 [4] J.A. Misewich et al., Science **300**, 783 (2003).
 [5] T. Ando, J. Phys. Soc. Japan **66**, 1066 (1996).
 [6] M. Rohlfing and S.G. Louie, Phys. Rev. B **62**, 4927 (2000).
 [7] W. Kohn and L.J. Sham, Phys. Rev. **140**, A1133 (1965).
 [8] M.S. Hybertsen and S.G. Louie, Phys. Rev. B **34**, 5390 (1986).
 [9] G. Strinati, Phys. Rev. B **29** 5718 (1984).
 [10] N. Troullier and J.L. Martins, Phys. Rev. **43**, 1993 (1991).
 [11] L. Kleinman and D.M. Bylander, Phys. Rev. Lett. **48**, 1425 (1982).
 [12] The influence of the dielectric background on the optical spectra of the metallic SWCNTs considered turned out to be negligible.
 [13] H. Ajiki and T. Ando, Physica B **201**, 349 (1994).
 [14] S.G. Louie in *Topics in Computational Materials Science*, edited by C.Y. Fong (World Scientific, Singapore, 1997), pg. 96.
 [15] X. Blase, L.X. Benedict, E.L. Shirley, S.G. Louie, Phys. Rev. Lett. **72** 1878 (1994).
 [16] R. Saito, M. Fujita, G. Dresselhaus, M. S Dresselhaus, Appl. Phys. Lett. **60**, 2204 (1992).
 [17] N. Hamada, S.I. Sawada, A. Oshiyama, Phys. Rev. Lett. **68**, 1579 (1992).
 [18] H.J. Liu and C.T. Chan, Phys. Rev. B **66**, 115416 (2002).
 [19] M. Machon, S. Reich, C. Thomsen, D. Sanchez-Portal, P. Ordejon, Phys. Rev. B **66**, 155410 (2002).
 [20] The calculation for the (8,0) tube (32 atoms in the unit cell) was already very challenging. We are currently studying the (4,2) tube (56 atoms in the unit cell), but this is a far more difficult calculation. The calculations scale as the number of atoms to the 4th power.
 [21] R. Loudon, Am. J. Phys. **27**, 649 (1959).
 [22] U. Fano, Phys. Rev. **124**, 1866 (1961).
 [23] R.B. Weisman and S.M. Bachilo, to be published.
 [24] M. Ichida, S. Mizuno, Y. Tani, Y. Saito, A. Nakamura, J. Phys. Soc. Jpn. **68**, 3131 (1999).
 [25] X. Liu et al., Phys. Rev. B **66**, 045411 (2002).
 [26] C.L. Kane and E.J. Mele, Phys. Rev. Lett. **90**, 207401 (2003).

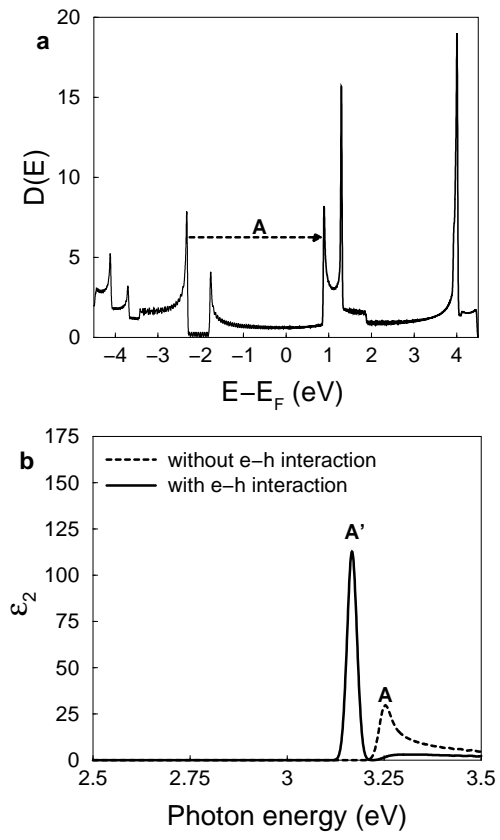


FIG. 1: Calculated quasiparticle DOS (a) and absorption spectra (b) for the (3,3) SWCNTs in $AlPO_4$ zeolite. Spectra are broadened with a Gaussian factor of 0.0125 eV.

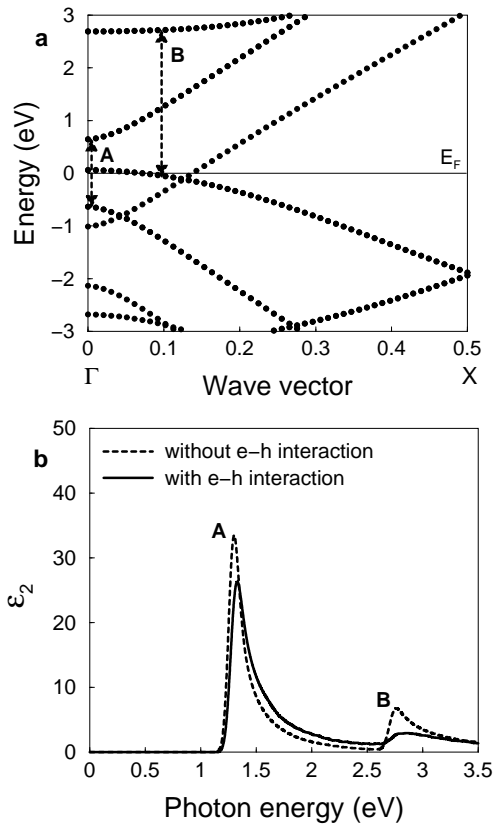


FIG. 2: Quasiparticle band structure (a) and absorption spectra (b) for the (5,0) SWCNTs in $AlPO_4$ zeolite.

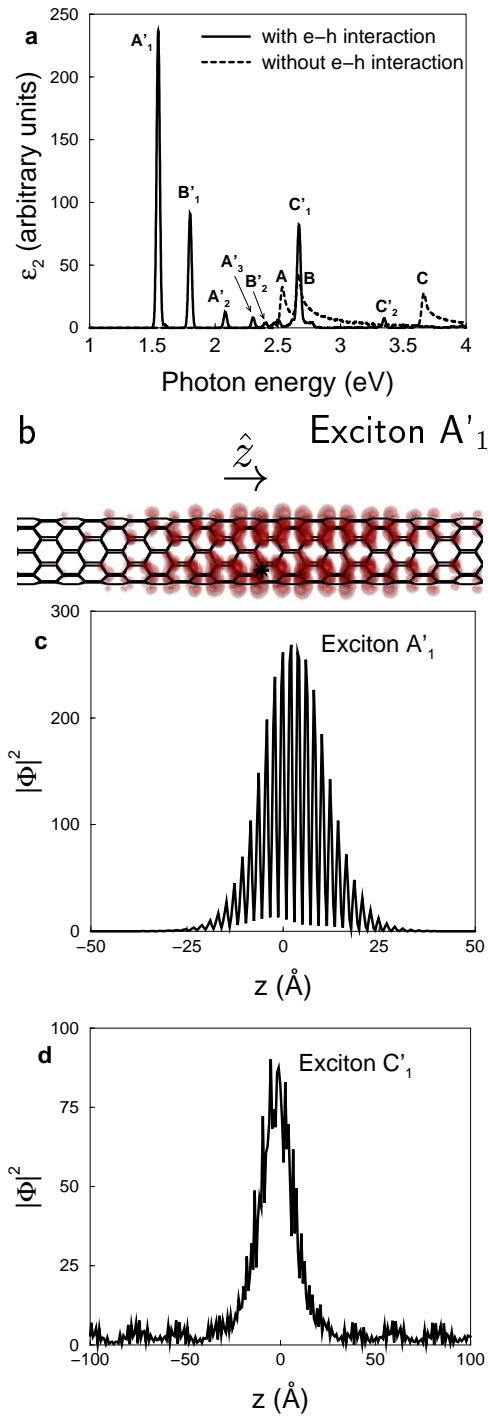


FIG. 3: Absorption spectra (a) and exciton wavefunctions (b,c,d) for the (8,0) SWCNT. Spectra are broadened with a Gaussian factor of 0.0125 eV.